The Method of Intelligent Image Processing Based on a Three-Channel Purely Convolutional Neural Network

Eugene Fedorov[1[0000-0003-3841-7373]], Valentyna Lukashenko[1[0000-0002-6749-9040]],

Volodymyr Patrushev[2[0000-0002-4061-4424]], Andriy Lukashenko[3[0000-0002-6016-1819]],

Kostiantyn Rudakov[1[0000-0003-0000-6077]], and Serhii Mitsenko[1[0000-0002-9582-7486]]

[1] Cherkasy State Technological University, Cherkasy, Shevchenko blvd., 460, 18006, Ukraine
{ckc, k.rudakov, s.mitsenko}@chdtu.edu.ua, fedorovee75@ukr.net
[2] Donetsk National Technical University, Pokrovsk, Shybankova sq., 2, 85300, Ukraine
wa_pat@ukr.net
[3] Institute of Electric Welding E. O. Paton, Kyiv, Bozhenko str., 11, 03680, Ukraine
ineks-kiev@ukr.net

Abstract. In the paper a method of intelligent image processing have been developed. This method based on a three channel purely convolutional neural network. The method consists of neural network model, a criterion to evaluate the effectiveness of the proposed model, a method for neural network learning in batch mode and a corresponding learning algorithm. This algorithm is intended for implementation on GPU by means of CUDA technology. The created model of neural network does not require the determination of the number of planes in hidden layers. This feature of the model simplifies its parametric identification "in large" and provides the use of three planes in the input layer. This simplifies the work with RGB images. The proposed method of intelligent image processing can be used in various intelligent systems of medical diagnostics.

Keywords: three-channel purely convolutional neural network, image recognition, batch learning mode, medical diagnostics, CUDA technologies.

1 Introduction

Currently, methods of automatic detection of mammary gland microcalcifications [1-2], nodes in the lungs [3]; polyps [4], pulmonary embolism [5]; brain tumors [6], etc., which are based on the approaches of artificial intelligence and are applied to digital images, are widely disseminated.

For image recognition, such approaches as [7]:

- metric [8, 9], which uses the metric to match the recognized and reference images;
- Bayesian [10], which uses a posteriori probability to match the recognized and reference images;
- generative [11-13], which uses a combination of a state machine and dynamic programming;

- neural [14-16], which uses an artificial neural network, are commonly used.

The highest probability of image recognition is achieved by means of deep neural networks.

Currently, the following deep neural networks are commonly used for image recognition:

- convolutional neural network (CNN) [17-18], which is a dynamic network;
- deep Boltzmann machine (DBM) [19-20], which is a recurrent network;
- deep autocoder [21], which is a static network;
- neocognitron [22], which is a dynamic network.

Compared with other deep neural networks, CNN has two advantages at the same time – the possibility of a batch learning mode and the highest probability of recognition.

The disadvantages of traditional CNN include the lack of binding of its learning procedure to a parallel architecture, the lack of automatic determination of the number of planes in its hidden layers, the consideration of its learning procedure for only one plane of the input layer. In this regard, it is relevant to create a modified CNN, which will eliminate these drawbacks.

The goal of the work is to create a method of intelligent image processing based on three-channel purely convolutional neural network. To achieve the goal, the following tasks have been set and solved:

1. to create a model of three-channel purely convolutional neural network;
2. to choose a criterion for evaluating the effectiveness of the proposed model;
   to develop a method for learning a three-channel purely convolutional neural network in batch mode;
3. to create a learning algorithm for three-channel purely convolutional neural network in batch mode, designed for implementation on GPU by means of CUDA technology;
4. to conduct a numerical study.

2 The creation of a model of three-channel purely convolutional neural network

In this paper a modification of CNN – three-channel purely convolutional neural network (3PCNN) – is offered. An example of 3PCNN for a feature matrix of 29x29 in size for three color components is shown in Fig. 1. Geometrically, communication area for the input, first, and second convolutional layers is a 3x3 square.

Unlike usual CNN, the proposed 3PCNN has the following features:

- there are three consecutive convolutional layers;
- the third convolutional layer replaces subsampling layer (communication area is shifted not by 1, but by q);
- the number of planes for the input and convolutional layers is three;

- each plane of the input layer is associated with only one plane of the first convolutional layer;
- each plane of the first convolutional layer is associated with only one plane of the second convolutional layer;
- each plane of the second convolutional layer is associated with only one plane of the third convolutional layer.

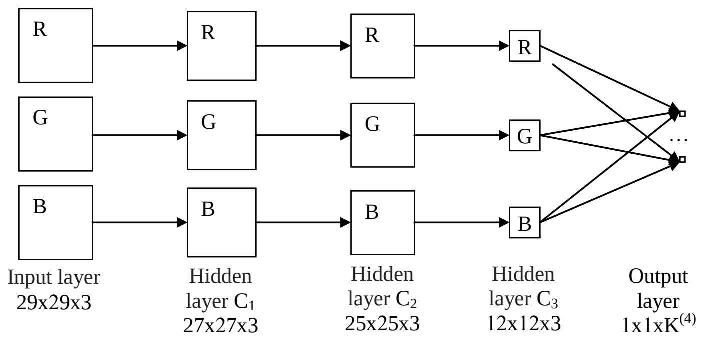

Fig. 1. Three-channel purely convolutional neural network (3PCNN).

The 3PCNN model is presented as follows:

$$u^{(0)}(m,k)=x(m,k)\,,\; m\in\{1,...,N/2\}^2\,,\;\; k\in\overline{1,3}\,,$$

$$u^{(1)}(m,k)=\,f^{(1)}(h^{(1)}(m,k))\,,\;\; m\in\{1,...,N^{(1)}\}^2\,,\;\; k\in\overline{1,3}\,,$$

$$h^{(1)}(m,k)=b^{(1)}(k)+\sum_{v}w^{(1)}(v,k,k)u^{(0)}(m+v,k)\,,\;\; v\in V_m^{(0)}\,,$$

$$u^{(2)}(m,k)=\,f^{(2)}(h^{(2)}(m,k))\,,\;\; m\in\{1,...,N^{(2)}\}^2\,,\;\; k\in\overline{1,3}\,,$$

$$h^{(2)}(m,k)=b^{(2)}(k)+\sum_{v}w^{(2)}(v,k,k)u^{(1)}(m+v,k)\,,\;\; v\in V_m^{(1)}\,,$$

$$u^{(3)}(m,k)=\,f^{(3)}(h^{(3)}(m,k))\,,\;\; m\in\{1,...,N^{(3)}\}^2\,,\;\; k\in\overline{1,3}\,,$$

$$h^{(3)}(m,k)=b^{(3)}(k)+\sum_{\upsilon}w^{(3)}(v,k,k)u^{(3)}(qm+\upsilon-(1-q,1-q),k)\,,\;\; v\in V_m^{(2)}\,,$$

$$u^{(4)}(i)=\,f^{(4)}(h^{(4)}(i))\,,\;\; i\in\overline{1,K^{(4)}}\,,$$

$$h^{(4)}(i)=b^{(4)}(i)+\sum_{k=1}^{3}\sum_{m}w^{(4)}(m,k,i)u^{(3)}(m,k)\,,\;\; m\in\{1,...,N^{(3)}\}^2\,,$$

where i – the number of the plane of output layer cells,

k – the number of the plane of convolutional layer cells C_1, C_2, C_3,

q – subsampling coefficient, which is a natural number,

ν – position in communication area, $\nu = (\nu_x, \nu_y)$,

$V_m^{(l)}$ – communication area of the l th layer for the neuron in m position of the $l+1$ st layer,

$K^{(4)}$ – the number of cell planes in the output layer,

$b^{(1)}(k)$ – threshold values for the neuron in m position of the k th plane of C_1 layer,

$b^{(2)}(k)$ – threshold values for the neuron in m position of the k th plane of C_2 layer,

$b^{(3)}(k)$ – threshold values for the neuron in m position of the k th plane of C_3 layer,

$b^{(4)}(i)$ – threshold values for the neuron of the i th plane of the output layer,

$w^{(1)}(\nu, k, k)$ – connection weight from the neuron in $m+\nu$ position of the k th plane of the input layer to the neuron in m position of the k th plane of C_1 layer,

$w^{(2)}(\nu, k, k)$ – connection weight from the neuron in $m+\nu$ position of the k th plane of C_1 layer to the neuron in m position of the k th plane of C_2 layer,

$w^{(3)}(\nu, k, k)$ – connection weight from the neuron in $qm+\upsilon-(1-q, 1-q)$ position of the k th plane of C_2 layer to the neuron in m position of the k th plane of C_3 layer,

$w^{(4)}(m, k, i)$ – connection weight from the neuron in m position of the k th plane of C_3 layer to the neuron of the i th plane of the output layer,

$u^{(1)}(m, k)$ – neuron yield in m position of the k th plane of C_1 layer,

$u^{(2)}(m, k)$ –neuron yield in m position of the k th plane of C_2 layer,

$u^{(3)}(m, k)$ – neuron yield in m position of the k th plane of C_3 layer,

$u^{(4)}(i)$ – neuron yield of the i th plane of the output layer,

$f^{(1)}$ – the ReLU function of neurons activation in C_1 layer,

$f^{(2)}$ – the ReLU function of neurons activation in C_2 layer,

$f^{(3)}$ – the ReLU function of neurons activation in C_3 layer,

$f^{(4)}$ – the logistic function of neurons activation in the output layer.

3 The choice of the criterion for evaluation of the proposed model effectiveness

In the work, for 3PCNN model learning the goal function is chosen, that means the choice of such parameter values, which deliver the minimum of root-mean-square error (the difference of model output and test output):

$$F = \frac{1}{PK^{(4)}} \sum_{\mu=1}^{P} \sum_{i=1}^{K^{(4)}} (u_{\mu}^{(4)}(i) - d_{\mu i})^2 \to \min_{W} \qquad (1)$$

where $u_{\mu}^{(4)} = (u_{\mu}^{(4)}(1),...,u_{\mu}^{(4)}(K^{(4)}))$ – the μ th model output signal,

$d_{\mu} = (d_{\mu 1},...,d_{\mu K^{(4)}})$ – the μ th test output signal,

P – test set power,

W – 3PCNN parameters, $W = \left\{ w^{(1)}(\nu,k,k),\ w^{(2)}(\nu,k,k),\ w^{(3)}(k,k),\ \ w^{(4)}(m,k,i) \right\}$.

4 The development of learning method for three-channel purely convolutional neural network in batch mode

In this paper, for 3PCNN an error correction learning (teacher learning), using the back propagation method (BP), is used. This is an iterative gradient learning method which minimizes root-mean-square error. In this paper, batch learning mode for parallel computing is offered.

The structure of the method for 3PCNN learning in batch mode is presented in Fig. 2.

The method for 3PCNN learning in batch mode consists of the following blocks.

Block 1 – initialize 3PCNN parameters

Set the number of the current learning era n by one.

$$b^{(1)}(n,k) = rand(),\ k \in \overline{1,3},$$

$$w^{(1)}(n,\nu,k,k) = rand(),\ \nu \in V^{(0)},\ k \in \overline{1,3},$$

$$b^{(2)}(n,k) = rand(),\ k \in \overline{1,3},$$

$$w^{(2)}(n,\nu,k,k) = rand(),\ \nu \in V^{(1)},\ k \in \overline{1,3},$$

$$b^{(3)}(n,k) = rand(),\ k \in \overline{1,3},$$

$$w^{(3)}(n,\nu,k,k) = rand(),\ \nu \in V^{(2)},\ k \in \overline{1,3},$$

$$b^{(4)}(n,i) = rand(),\ i \in \overline{1,K^{(4)}},$$

$$w^{(4)}(n,m,k,i) = rand(),\ m \in \{1,...,N^{(3)}\}^2,\ k \in \overline{1,3},\ i \in \overline{1,K^{(4)}},$$

where $V^{(l)}$ – communication area in the l th layer.

Block 2 – Specify the learning set

$$\{(\mathbf{x}_\mu, \mathbf{d}_\mu) \mid \mathbf{x}_\mu \in R^{(N/2)\times(N/2)}, \mathbf{d}_\mu \in \{0,1\}^{K^{(4)}}\},\ \mu \in \overline{1,P},$$

where $\mathbf{x}_\mu$ – the μ th learning input matrix of features,

$\mathbf{d}_\mu$ – the μ th learning output vector,

P – learning set power.

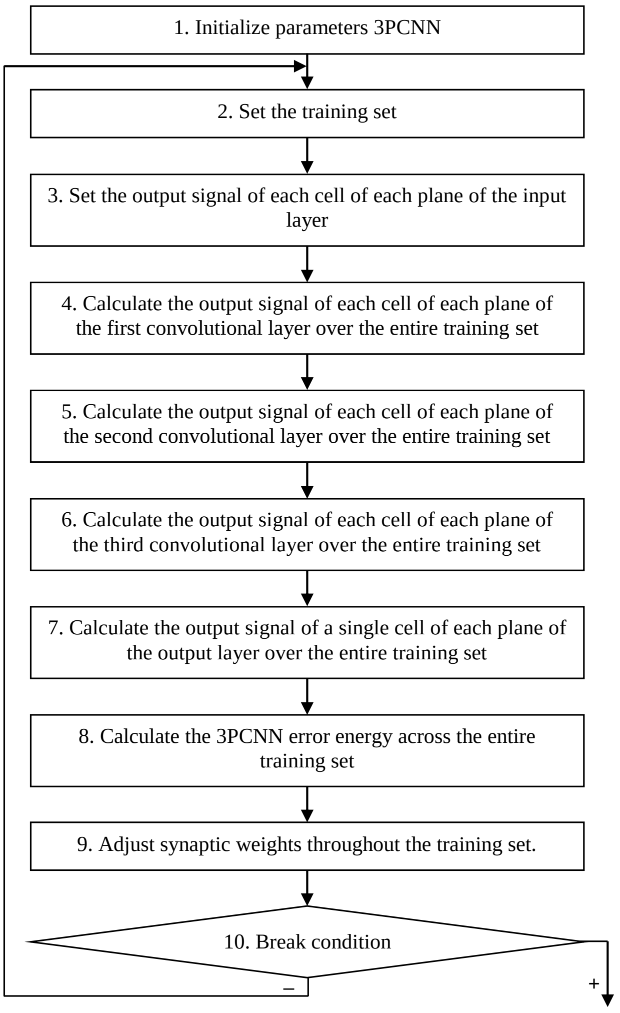
1. Initialize parameters 3PCNN
2. Set the training set
3. Set the output signal of each cell of each plane of the input layer
4. Calculate the output signal of each cell of each plane of the first convolutional layer over the entire training set
5. Calculate the output signal of each cell of each plane of the second convolutional layer over the entire training set
6. Calculate the output signal of each cell of each plane of the third convolutional layer over the entire training set
7. Calculate the output signal of a single cell of each plane of the output layer over the entire training set
8. Calculate the 3PCNN error energy across the entire training set
9. Adjust synaptic weights throughout the training set.
10. Break condition
–
+

Fig. 2. The structure of the method for 3PCNN learning in batch mode.

Block 3 – Set the output signal of each cell of each plane of the input layer

$$u_\mu^{(0)}(n,m,k) = x_\mu(m,k),\ m \in \{1,...,N/2\}^2,\ k \in \overline{1,3},\ \mu \in \overline{1,P}.$$

Block 4 – Calculate the output signal of each cell of each plane of the first convolutional layer over the entire learning set

$$u_\mu^{(1)}(n,m,k) = f^{(1)}(h_\mu^{(1)}(n,m,k)),\ m \in \{1,...,N^{(1)}\}^2,\ k \in \overline{1,3},\ \mu \in \overline{1,P},$$

$$h_\mu^{(1)}(n,m,k) = b^{(1)}(n,k) + \sum_\nu w^{(1)}(n,\nu,k,k) u_\mu^{(0)}(n,m+\nu,k),\ \nu \in V_m^{(0)}.$$

Block 5 – Calculate the output signal of each cell of each plane of the second convolutional layer over the entire learning set

$$u_\mu^{(2)}(n,m,k) = f^{(2)}(h_\mu^{(2)}(n,m,k)),\ m \in \{1,...,N^{(2)}\}^2,\ k \in \overline{1,3},\ \mu \in \overline{1,P},$$

$$h_\mu^{(2)}(n,m,k) = b^{(2)}(n,k) + \sum_\nu w^{(2)}(n,\nu,k,k) u_\mu^{(1)}(n,m+\nu,k),\ \nu \in V_m^{(1)}.$$

Block 6 – Calculate the output signal of each cell of each plane of the third convolutional layer over the entire learning set

$$u_\mu^{(3)}(n,m,k) = f^{(3)}(h_\mu^{(3)}(n,m,k)),\ m \in \{1,...,N^{(3)}\}^2,\ k \in \overline{1,3},\ \mu \in \overline{1,P},$$

$$h_\mu^{(3)}(n,m,k) = b^{(3)}(n,k) + \sum_\upsilon w^{(3)}(n,\nu,k,k) u^{(2)}(n,qm+\upsilon-(1-q,1-q),k),\ \nu \in V_m^{(2)}.$$

Block 7 – Calculate the output signal of a single cell of each plane of the output layer over the entire learning set

$$u_\mu^{(4)}(n,i) = f^{(4)}(h_\mu^{(4)}(n,i)),\ i \in \overline{1,K^{(4)}},\ \mu \in \overline{1,P},$$

$$h_\mu^{(4)}(n,i) = b^{(4)}(n,i) + \sum_{k=1}^{3}\sum_m w^{(4)}(n,m,k,i) u_\mu^{(3)}(n,m,k),\ m \in \{1,...,N^{(3)}\}^2.$$

Block 8 – Calculate the energy of 3PCNN error over the entire learning set

$$E(n) = \frac{1}{2P}\sum_{\mu=1}^{P}\sum_{i=1}^{K^{(4)}} e_{\mu i}^2(n),\ e_{\mu i}(n) = u_\mu^{(4)}(n,i) - d_{\mu i}.$$

Block 9 – Adjust synaptic weights based on generalized delta rule over the entire learning set

$$b^{(4)}(n+1,i) = b^{(4)}(n,i) - \eta(n)\frac{\partial E(n)}{\partial b^{(4)}(n,i)},\ i \in \overline{1,K^{(4)}},$$

$$w^{(4)}(n+1,m,k,i)=w^{(4)}(n,m,k,i)-\eta(n)\frac{\partial E(n)}{\partial w^{(4)}(n,m,k,i)},\ m\in\{1,...,N^{(3)}\}^2,\ k\in\overline{1,3},\ i\in\overline{1,K^{(4)}},$$

$$b^{(3)}(n+1,k)=b^{(3)}(n,k)-\eta(n)\frac{\partial E(n)}{\partial b^{(3)}(n,k)},\ k\in\overline{1,3},$$

$$w^{(3)}(n+1,\nu,k,k)=w^{(3)}(n,\nu,k,k)-\eta(n)\frac{\partial E(n)}{\partial w^{(3)}(n,\nu,k,k)},\ \nu\in V^{(2)},\ k\in\overline{1,3},$$

$$b^{(2)}(n+1,k)=b^{(2)}(n,k)-\eta(n)\frac{\partial E(n)}{\partial b^{(2)}(n,k)},\ k\in\overline{1,3},$$

$$w^{(2)}(n+1,\nu,k,k)=w^{(2)}(n,\nu,k,k)-\eta(n)\frac{\partial E(n)}{\partial w^{(2)}(n,\nu,k,k)},\ \nu\in V^{(1)},\ k\in\overline{1,3},$$

$$b^{(1)}(n+1,k)=b^{(1)}(n,k)-\eta(n)\frac{\partial E(n)}{\partial b^{(1)}(n,k)},\ k\in\overline{1,3},$$

$$w^{(1)}(n+1,\nu,k,k)=w^{(1)}(n,\nu,k,k)-\eta(n)\frac{\partial E(n)}{\partial w^{(1)}(n,\nu,k,k)},\ \nu\in V^{(0)},\ k\in\overline{1,3},$$

$$\frac{\partial E(n)}{\partial b^{(4)}(n,i)}=\frac{1}{P}\sum_{\mu=1}^{P}g_{\mu}^{(4)}(n,i),$$

$$\frac{\partial E(n)}{\partial w^{(4)}(n,m,k,i)}=\frac{1}{P}\sum_{\mu=1}^{P}u_{\mu}^{(3)}(n,m,k)g_{\mu}^{(4)}(n,i),$$

$$\frac{\partial E(n)}{\partial b^{(3}(n,k)}=\frac{1}{P}\sum_{\mu=1}^{P}\sum_{m}g_{\mu}^{(3)}(n,m,k),\ m\in\{1,...,N^{(2)}\}^2,$$

$$\frac{\partial E(n)}{\partial w^{(3)}(n,\nu,k,k)}=\frac{1}{P}\sum_{\mu=1}^{P}\sum_{m}u_{\mu}^{(2)}(n,qm+\upsilon+(1-q,1-q),k)g_{\mu}^{(3)}(n,m,k),\ m\in\{1,...,N^{(2)}\}^2,$$

$$\frac{\partial E(n)}{\partial b^{(2)}(n,k)}=\frac{1}{P}\sum_{\mu=1}^{P}\sum_{m}g_{\mu}^{(2)}(n,m,k),\ m\in\{1,...,N^{(1)}\}^2,$$

$$\frac{\partial E(n)}{\partial w^{(2)}(n,\nu,k,k)}=\frac{1}{P}\sum_{\mu=1}^{P}\sum_{m}u_{\mu}^{(1)}(n,m+\nu,k)g_{\mu}^{(2)}(n,m,k),\ m\in\{1,...,N^{(1)}\}^2,$$

$$\frac{\partial E(n)}{\partial b^{(1)}(n,k)}=\frac{1}{P}\sum_{\mu=1}^{P}\sum_{m}g_{\mu}^{(1)}(n,m,k),\ m\in\{1,...,N/2\}^2,$$

$$\frac{\partial E(n)}{\partial w^{(1)}(n,\nu,k,k)} = \frac{1}{P}\sum_{\mu=1}^{P}\sum_{m} u_{\mu}^{(0)}(n,m+\nu,k) g_{\mu}^{(1)}(n,m,k)\,,\ m \in \{1,...,N/2\}^2\,,$$

$$g_{\mu}^{(4)}(n,i) = e_{\mu i}(n) f'^{(4)}(h_{\mu}^{(4)}(n,i))\,,$$

$$g_{\mu}^{(3)}(n,m,k) = f'^{(3)}(h_{\mu}^{(3)}(n,m,k))\sum_{i=1}^{K^{(4)}} w^{(4)}(n,m,k,i) g_{\mu}^{(4)}(n,i)\,,$$

$$g_{\mu}^{(2)}(n,m,k) = f'^{(2)}(h_{\mu}^{(2)}(n,m,k))\cdot$$

$$\cdot\sum_{\nu} w^{(3)}(n,\nu,k,k) g_{\mu}^{(3)}\left(n, \left[\frac{m-\nu-(1,1)}{q}\right]+(1,1),k\right),\ \nu \in D_m^{(3)}\,,$$

$$g_{\mu}^{(1)}(n,m,k) = f'^{(1)}(h_{\mu}^{(1)}(n,m,k))\sum_{\nu} w^{(2)}(n,\nu,k,k) g_{\mu}^{(2)}(n,m-\nu,k)\,,\ \nu \in D_m^{(2)}\,,$$

where $D_m^{(l)}$ – communication area of the l th layer for the neuron in m position of the $l-1$ th layer,

$\eta(n)$ – parameter that determines the learning rate in accordance with the rule of exponential decay,

$$\eta(n) = \eta(0)e^{-decay\_rate\cdot t}\,;\ decay\_rate > 0\,,$$

where $\eta(0)$ – initial learning rate, $\eta(0) > 0$.

Block 10 – Check termination condition.

If $E(n) \geq \varepsilon$, then increase the number of the era n by one and go to block 2.

5 The creation of learning algorithm of three-channel purely convolutional neural network in batch mode

The algorithm for 3PCNN learning in batch mode, designed for implementation on GPU by means of CUDA technology, is shown in Fig. 3. This block diagram functions as follows.

Step 1 – Download the initial values of 3PCNN parameters into GPU global memory.

Step 2 – Download the learning set into GPU global memory.

Step 3 – Download the output signal of each cell of each plane of the input layer into GPU global memory.

Step 4 – Calculate the output signal of each cell of each plane of the first convolutional layer $u_{\mu}^{(1)}(n,m,k)$ over the entire learning set using $3P(N^{(1)})^2$ threads which are grouped into $\left(3P(N^{(1)})^2\right)/N^s$ blocks, where N^s – the number of threads in the block. Each thread computes

$$u_\mu^{(1)}(n,m,k) = f^{(1)}(h_\mu^{(1)}(n,m,k)),$$

$$h_\mu^{(1)}(n,m,k) = b^{(1)}(n,k) + \sum_\nu w^{(1)}(n,\nu,k,k)u_\mu^{(0)}(n,m+\nu,k),\ \nu \in V_m^{(0)}.$$

Step 5 – Calculate the output signal of each cell of each plane of the second convolutional layer $u_\mu^{(2)}(n,m,k)$ over the entire learning set using $3P(N^{(2)})^2$ threads which are grouped into $\left(3P(N^{(2)})^2\right)/N^s$ blocks. Each thread computes

$$u_\mu^{(2)}(n,m,k) = f^{(2)}(h_\mu^{(2)}(n,m,k)),$$

$$h_\mu^{(2)}(n,m,k) = b^{(2)}(n,k) + \sum_\nu w^{(2)}(n,\nu,k,k)u_\mu^{(1)}(n,m+\nu,k),\ \nu \in V_m^{(0)}.$$

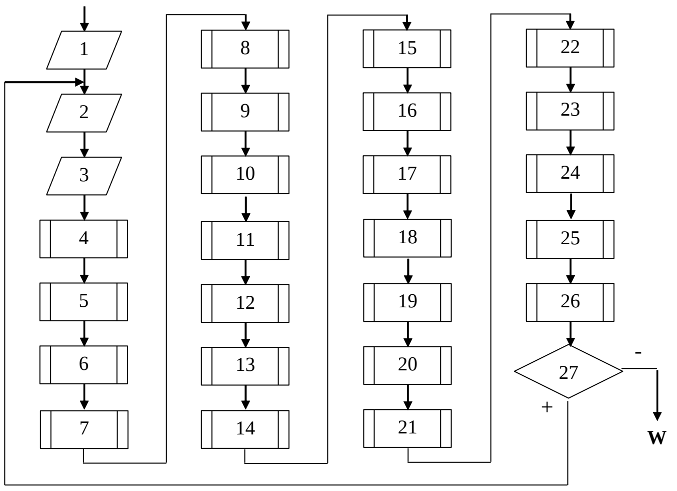

Fig. 3. Block diagram of the algorithm for 3PCNN learning in batch mode.

Step 6 – Calculate the output signal of each cell of each plane of the third convolutional layer $u_\mu^{(3)}(n,m,k)$ over the entire learning set using $3P(N^{(2)})^2$ threads which are grouped into $\left(3P(N^{(2)})^2\right)/N^s$ blocks. Each thread computes

$$u_\mu^{(3)}(n,m,k) = f^{(3)}(h_\mu^{(3)}(n,m,k)),$$

$$h_\mu^{(3)}(n,m,k) = b^{(3)}(n,k) + \sum_\upsilon w^{(3)}(n,\nu,k,k)u^{(2)}(n,qm+\upsilon-(1-q,1-q),k),\ \nu \in V_m^{(2)}.$$

Step 7 – Calculate the $s_\mu(n,i)$ sum over the entire learning set using $3P(N^{(3)})^2K^{(4)}$ threads which are grouped into $\left(3P(N^{(3)})^2K^{(4)}\right)/N^s$ blocks. In each block, based on the reduction, a partial sum from N^s elements of the $w^{(4)}(n,m,k,i)u_\mu^{(3)}(n,m,k)$ form is calculated. Partial sums, received in each block, are added up, based on the reduction.

Step 8 – Calculate the output signal of a single cell of each plane of the output $u_\mu^{(4)}(n,i)$ layer over the entire learning set using $PK^{(4)}$ threads which are grouped into $\left(PK^{(4)}\right)/N^s$ blocks. Each thread computes

$$u_\mu^{(4)}(n,i) = f^{(4)}(h_\mu^{(4)}(n,i)),$$

$$h_\mu^{(4)}(n,i) = b^{(4)}(n,i) + s_\mu(n,i).$$

Step 9 – Calculate the energy of error $E(n)$ over the entire learning set using $PK^{(4)}$ threads which are grouped into $\left(PK^{(4)}\right)/N^s$ blocks. In each block, based on the reduction, a partial sum from N^s elements of the $u_\mu^{(4)}(n,i) - d_{\mu i}$ form is calculated. Partial sums, received in each block, are added, based on the reduction, and the result is divided by $2P$.

Step 10 – Calculate the partial derivative $\dfrac{\partial E(n)}{\partial b^{(4)}(n,i)}$ over the entire learning set using $PK^{(4)}$ threads which are grouped into $\left(PK^{(4)}\right)/N^s$ blocks. In each block, based on the reduction, a partial sum from N^s elements of the $g_\mu^{(4)}(n,i) = e_{\mu i}(n) f'^{(4)}(h_\mu^{(4)}(n,i))$ form is calculated. Partial sums, received in each block, are added, based on the reduction, and the result is divided by P.

Step 11 – Calculate the threshold value $b^{(4)}(n+1,i)$ using $K^{(4)}$ threads which are grouped into one block. Each thread computes

$$b^{(4)}(n+1,i) = b^{(4)}(n,i) - \eta(n)\frac{\partial E(n)}{\partial b^{(4)}(n,i)}.$$

Step 12 – Calculate the partial derivative $\dfrac{\partial E(n)}{\partial w^{(4)}(n,m,k,i)}$ over the entire learning set using $3P(N^{(3)})^2K^{(4)}$ threads which are grouped into $\left(3P(N^{(3)})^2K^{(4)}\right)/N^s$ blocks. In each block, based on the reduction, a partial sum from N^s elements of the $u_\mu^{(3)}(n,m,k)g_\mu^{(4)}(n,i)$ form is calculated. Partial sums, received in each block, are added, based on the reduction, and the result is divided by P.

Step 13 – Calculate synaptic weight $w^{(4)}(n+1,m,k,i)$ using $3(N^{(3)})^2 K^{(4)}$ threads which are grouped into $\left(3(N^{(3)})^2 K^{(4)}\right)\big/N^s$ blocks. Each thread computes

$$w^{(4)}(n+1,m,k,i) = w^{(4)}(n,m,k,i) - \eta(n)\frac{\partial E(n)}{\partial w^{(4)}(n,m,k,i)}.$$

Step 14 – Calculate the partial derivative $\frac{\partial E(n)}{\partial b^{(3)}(n,k)}$ over the entire learning set using $3P(N^{(2)})^2$ threads which are grouped into $\left(3P(N^{(2)})^2\right)\big/N^s$ blocks. In each block, based on the reduction, a partial sum from N^s elements of the $g_\mu^{(3)}(n,m,k) = f'^{(3)}(h_\mu^{(3)}(n,m,k))\sum_{i=1}^{K^{(4)}} w^{(4)}(n,m,k,i)g_\mu^{(4)}(n,i)$ form is calculated. Partial sums, received in each block, are added, based on the reduction, and the result is divided by P.

Step 15 – Calculate the threshold value $b^{(3)}(n+1,k)$ using three threads, which are grouped into one block. Each thread computes

$$b^{(3)}(n+1,k) = b^{(3)}(n,k) - \eta(n)\frac{\partial E(n)}{\partial b^{(3)}(n,k)}.$$

Step 16 – Calculate the partial derivative $\frac{\partial E(n)}{\partial w^{(3)}(n,\nu,k,k)}$ over the entire learning set using $3P(N^{(2)})^2\,|V^{(2)}|$ threads which are grouped into $\frac{3P(N^{(2)})^2\,|V^{(2)}|}{N^s}$ blocks. In each block, based on the reduction, a partial sum from N^s elements of the $u_\mu^{(2)}(n,qm+\upsilon+(1-q,1-q),k)g_\mu^{(3)}(n,m,k)$ form is calculated. Partial sums, received in each block, are added, based on the reduction, and the result is divided by P.

Step 17 – Calculate synaptic weight $w^{(3)}(n+1,\nu,k,k)$ using $3|V^{(2)}|$ threads which are grouped into one block. Each thread computes

$$w^{(3)}(n+1,\nu,k,k) = w^{(3)}(n,\nu,k,k) - \eta(n)\frac{\partial E(n)}{\partial w^{(3)}(n,\nu,k,k)}.$$

Step 18 – Calculate the partial derivative $\frac{\partial E(n)}{\partial b^{(2)}(n,k)}$ over the entire learning set using $3P(N^{(1)})^2$ threads which are grouped into $\left(3P(N^{(1)})^2\right)\big/N^s$ blocks. In each block, based on the reduction, a partial sum from N^s elements of the

$$g_{\mu}^{(2)}(n,m,k) = f'^{(2)}(h_{\mu}^{(2)}(n,m,k)) \cdot \sum_{\nu} w^{(3)}(n,\nu,k,k) g_{\mu}^{(3)}\left(n, \left[\frac{m-\nu-(1,1)}{q}\right] + (1,1), k\right)$$

form is calculated. Partial sums, received in each block, are added, based on the reduction, and the result is divided by P.

Step 19 – Calculate the threshold value $b^{(2)}(n+1,k)$ using three threads, which are grouped into one block. Each thread computes

$$b^{(2)}(n+1,k) = b^{(2)}(n,k) - \eta(n)\frac{\partial E(n)}{\partial b^{(2)}(n,k)}.$$

Step 20 – Calculate the partial derivative $\frac{\partial E(n)}{\partial w^{(2)}(n,\nu,k,k)}$ over the entire learning set using $3P(N^{(1)})^2 |V^{(1)}|$ threads which are grouped into $\frac{3P(N^{(1)})^2 |V^{(1)}|}{N^s}$ blocks. In each block, based on the reduction, a partial sum from N^s elements of the $u_{\mu}^{(1)}(n,m+\nu,k) g_{\mu}^{(2)}(n,m,k)$ form is calculated. Partial sums, received in each block, are added, based on the reduction, and the result is divided by P.

Step 21 – Calculate synaptic weight $w^{(2)}(n+1,\nu,k,k)$ using $3|V^{(1)}|$ threads which are grouped into one block. Each thread computes

$$w^{(2)}(n+1,\nu,k,k) = w^{(2)}(n,\nu,k,k) - \eta(n)\frac{\partial E(n)}{\partial w^{(2)}(n,\nu,k,k)}.$$

Step 22 – Calculate the partial derivative $\frac{\partial E(n)}{\partial b^{(1)}(n,k)}$ over the entire learning set using $3P(N/2)^2$ threads which are grouped into $\left(3P(N/2)^2\right)/N^s$ blocks. In each block, based on the reduction, a partial sum from N^s elements of the $g_{\mu}^{(1)}(n,m,k) = f'^{(1)}(h_{\mu}^{(1)}(n,m,k)) \sum_{\nu} w^{(2)}(n,\nu,k,k) g_{\mu}^{(2)}(n,m-\nu,k)$ form is calculated. Partial sums, received in each block, are added, based on the reduction, and the result is divided by P.

Step 23 – Calculate the threshold value $b^{(1)}(n+1,k)$ using three threads which are grouped into one block. Each thread computes

$$b^{(1)}(n+1,k) = b^{(1)}(n,k) - \eta(n)\frac{\partial E(n)}{\partial b^{(1)}(n,k)}.$$

Step 24 – Calculate the partial derivative $\frac{\partial E(n)}{\partial w^{(1)}(n,\nu,k,k)}$ over the entire learning set using $3P(N/2)^2|V^{(0)}|$ threads which are grouped into $\frac{3P(N/2)^2|V^{(0)}|}{N^s}$ blocks. In each block, based on the reduction, a partial sum from N^s elements of the $u_\mu^{(0)}(n,m+\nu,k)g_\mu^{(1)}(n,m,k)$ form is calculated. Partial sums, received in each block, are added, based on the reduction, and the result is divided by P.

Step 25 – Calculate synaptic weight $w^{(1)}(n+1,\nu,k,k)$ using $3|V^{(0)}|$ threads which are grouped into one block. Each thread computes

$$w^{(1)}(n+1,\nu,k,k)=w^{(1)}(n,\nu,k,k)-\eta(n)\frac{\partial E(n)}{\partial w^{(1)}(n,\nu,k,k)}.$$

Step 26 – Calculate learning speed

$$\eta(n)=\eta(0)e^{-decay\_rate\cdot t};\ decay\_rate>0.$$

Step 27 – Check termination condition.

If $E(n)\ge\varepsilon$, then increase the number of era n by one and go to step 2.

6 Numerical research

Recognition probabilities, obtained on the basis of CIFAR-10 based on traditional CNN and the proposed 3PCNN, are presented in Table 1. At the same time, traditional CNN had three stages (each consisted of a convolutional and subsampling layer with 5x5 and 2x2 communication areas, respectively), the first stage had four planes for each layer, the second stage had 16 planes for each layer, the third stage had 64 planes for each layer. The tests were carried out on GeForce 920M video card with the number of threads in the block $N^s=1024$.

According to Table 1, 3PCNN with image preprocessing gives the best results.

Table 1. Image recognition probability.

Neural networks	Recognition probability
CNN	0.97
3PCNN	0.98

Conclusions

1. To solve the problem of improving the quality of intelligent medical image processing, appropriate methods for image recognition have been investigated. These

studies have shown that the use of convolutional neural networks is currently the most effective.
2. The created model of three-channel purely convolutional neural network does not require the determination of the number of planes in hidden layers, that simplifies its parametric identification “in large” and ensures the use of three planes in the input layer, which simplifies the work with RGB images.
3. The created algorithm for learning a three-channel purely convolutional neural network is designed for software implementation on GPU by means of CUDA technology.
4. The proposed method of intelligent image processing, based on three-channel pure convolutional neural network, can be used in various intelligent systems of medical diagnostics.

References

1. Zhang, W., Doi, K., Giger, M., Wu, Y., Nishikawa, R., Schmidt, R.: Computerized detection of clustered microcalcifications in digital mammograms using a shift-invariant artificial neural network. In: Williamson, J. (eds.) Medical Physics, vol. 21, pp. 517–524, (1994) doi.org/10.1118/1.597177
2. Chan, H., Lo, S., Lam, S., Helvie, M.: Computer-aided detection of mammographic microcalcifications: Pattern recognition with an artificial neural network. In: Williamson, J. (eds.) Medical Physics, vol. 22, pp. 1555–1567, (1995) doi.org/10.1118/1.597428
3. Lo, S., Lou, S., Lin, J., Freedman, M., Chien, M., Mun, S.: Artificial convolution neural network techniques and applications for lung nodule detection. In: Insana, M. (eds.) Medical Imaging, IEEE Transactions, vol. 14, pp. 711–718, (1995) doi.org/10.1109/42.476112
4. Tajbakhsh, N., Gurudu, S, Liang, J.: A comprehensive computer-aided polyp detection system for colonoscopy videos. In: Ourselin, S., Alexander, D., Westin, C., Cardoso, M. (eds.) Information Processing in Medical Imaging. Springer, pp. 327–338, (2015) doi.org/10.1007/978-3-319-19992-4_25
5. Tajbakhsh, N., Liang, J.: Computer-aided pulmonary embolism detection using a novel vessel-aligned multi-planar image representation and convolutional neural networks. In: Navab, N., (eds.) MICCAI 2015, Part II, LNCS 9350, pp. 62–69 (2015) doi.org/10.1007/978-3-319-24571-3_8
6. Havaei, M., Davy, A., Warde-Farley, D., Biard, A., Courville, A., Bengio, Y., Pal C., Jodoin, P, Larochelle, H.: Brain tumor segmentation with deep neural networks. In: Medical Image Analysis, vol. 35, pp. 18–31, (2017) doi.org/10.1016/j.media.2016.05.004
7. Fedorov E., Tossoriteit E.: Models and methods of spectator images recognition. Donetsk: Knowledge (Donetsk branch), 422 pp. (2013) in Russian
8. Brunelli, R., Poggio, T.: Face recognition: features versus templates. In: IEEE Transactions on Pattern Analysis and Machine Intelligence, vol. 15, pp. 235–241, (1993) doi.org/10.1109/34.254061

9. Baron, R.: Mechanisms of human facial recognition. In: International Journal of Man-Machine Studies, vol. 15, pp. 137–178, (2008) doi.org/10.1016/S0020-7373(81)80001-6
10. Moghaddam, B., Jebara, T., Pentland, A.: Bayesian Face Recognition. In: Pattern recognition, vol. 33, pp. 1771–1782, (2000) doi.org/10.1016/S0031-3203(99)00179-X
11. Nefian, A., Hayes, M.: Hidden Markov models for face recognition. In: Proceedings of the 1998 IEEE International Conference on Acoustics, Speech and Signal Processing, ICASSP '98, pp. 2721–2724, (1998) doi.org/10.1109/ICASSP.1998.678085
12. Kohir, V., Desai, U.: Face recognition using DCT-HMM approach. In: Proceedings Fourth IEEE Workshop on Applications of Computer Vision. WACV'98, pp. 3400–3410, (1998) doi.org/10.1109/ACV.1998.732884
13. Daleno, D., Cariello, L., Giannini, M., Mastronardi, G.: Pseudo 2D hidden Markov model and neural network coefficients in face recognition. In: Oravec, M. (eds.) Face Recognition, pp. 151–170, (2010).
14. Tkachenko, R., Izonin, I.: Model and Principles for the Implementation of Neural-Like Structures based on Geometric Data Transformations. In: Hu, Z., Petoukhov, S., (eds) Advances in Computer Science for Engineering and Education. ICCSEEA2018. Advances in Intelligent Systems and Computing. Springer, Cham, vol.754, pp.578-587, (2018) doi.org/10.1007/978-3-319-91008-6_58
15. Lyubchyk, L., Bodyansky, E., Rivtis, A.: Adaptive harmonic components detection and forecasting in wave non-periodic time series using neural networks. In: ISCDMCI'2002. - Conf, pp. 433-435, (2002).
16. Subbotin, S.: The special deep neural network for stationary signal spectra classification. In: 2018 14th International Conference on Advanced Trends in Radioelectronics, Telecommunications and Computer Engineering, TCSET 2018 – Proceedings. (2018) doi.org/10.1109/TCSET.2018.8336170
17. LeCun, Y., Bengio, Y.: Convolutional networks for images, speech, and time series. In: Arbib, M. (eds.) The handbook of brain theory and neural networks, MIT Press Cambridge, pp. 255–258, (1998).
18. Lawrence, S., Giles, C., Tsoi, A., Back, A.: Face recognition: a convolutional neural network approach. In: IEEE Transactions on Neural Networks, vol. 8, pp. 98–113, (1997) doi.org/10.1109/72.554195
19. Salakhutdinov, R., Hinton, G.: Deep Boltzmann machines. Journal of Machine Learning Research, vol. 5, pp. 448–455, (2009).
20. Salakhutdinov, R., Larochelle, H.: Efficient learning of deep Boltzmann machines. In: Journal of Machine Learning Research, vol. 9, pp. 693–700, (2010).
21. Hinton, G., Salakhutdinov, R.: Reducing the dimensionality of data with neural networks. Science, vol. 313, pp. 504–507, (2006) doi.org/10.1126/science.1127647
22. Fukushima, K.: Neocognitron for handwritten digit recognition. Neurocomputing, vol. 51, pp. 161–180, (2003) doi.org/10.1016/S0925-2312(02)00614-8